A structural basis for drug-induced long QT syndrome

John S. Mitcheson*†, Jun Chen*, Monica Lin*, Chris Culberson‡, and Michael C. Sanguinetti*§

*Department of Internal Medicine, University of Utah, 15 N 2030 E, Room 4220, Salt Lake City, UT 84112; and ‡Molecular Systems, Merck Research Laboratories, P.O. Box 4, West Point, PA 19486

Edited by William A. Catterall, University of Washington School of Medicine, Seattle, WA, and approved August 14, 2000 (received for review May 26, 2000)

Mutations in the HERG K^+ channel gene cause inherited long QT syndrome (LQT), a disorder of cardiac repolarization that predisposes affected individuals to lethal arrhythmias [Curran, M. E., Splawski, I., Timothy, K. W., Vincent, G. M., Green, E. D. & Keating, M. T. (1995) *Cell* 80, 795–804]. Acquired LQT is far more common and is most often caused by block of cardiac HERG K^+ channels by commonly used medications [Roden, D. M., Lazzara, R., Rosen, M., Schwartz, P. J., Towbin, J. & Vincent, G. M. (1996) *Circulation* 94, 1996–2012]. It is unclear why so many structurally diverse compounds block HERG channels, but this undesirable side effect now is recognized as a major hurdle in the development of new and safe drugs. Here we use alanine-scanning mutagenesis to determine the structural basis for high-affinity drug block of HERG channels by MK-499, a methanesulfonanilide antiarrhythmic drug. The binding site, corroborated with homology modeling, is comprised of amino acids located on the S6 transmembrane domain (G648, Y652, and F656) and pore helix (T623 and V625) of the HERG channel subunit that face the cavity of the channel. Other compounds that are structurally unrelated to MK-499, but cause LQT, also were studied. The antihistamine terfenadine and a gastrointestinal prokinetic drug, cisapride, interact with Y652 and F656, but not with V625. The aromatic residues of the S6 domain that interact with these drugs (Y652 and F656) are unique to eag/erg K^+ channels. Other voltage-gated K^+ (Kv) channels have Ile and Val (Ile) in the equivalent positions. These findings suggest a possible structural explanation for how so many commonly used medications block HERG but not other Kv channels and should facilitate the rational design of drugs devoid of HERG channel binding activity.

Long QT syndrome (LQT) is an abnormality of cardiac muscle repolarization that predisposes affected individuals to a ventricular arrhythmia that can degenerate into ventricular fibrillation and cause sudden death (1). The cellular mechanism of the lengthened QT interval recorded on the body surface electrocardiogram is prolonged ventricular action potentials. Recent genetic discoveries have determined that the molecular mechanism of inherited LQT is mutations in one of several genes [e.g., *HERG* (2), *KCNE2* (3)] that encode ion channel subunits important for normal repolarization of the ventricle. *HERG* encodes the pore-forming subunits of channels that conduct the rapid delayed rectifier K^+ current (I_{Kr}; refs. 4 and 5). LQT also can be acquired as a side effect of treatment with commonly used medications, including some antiarrhythmic, antihistamine, antibiotic, psychoactive, and gastrointestinal prokinetic agents (6, 7). Although drug-induced LQT theoretically could result from reduction of any voltage-gated K^+ current that contributes to ventricular repolarization, all known drugs with this side effect preferentially block I_{Kr} (1, 8, 9). It is unclear why so many structurally diverse compounds block HERG channels, but this undesirable side effect now is recognized as a major hurdle in the development of new and safe drugs (9, 10). Previous studies have characterized single residues of HERG that when mutated altered the sensitivity of the channel to block by the methanesulfonanilide antiarrhythmic drug dofetilide. However, these residues are believed to alter drug binding by an allosteric effect related to the loss of inactivation gating (11). A more recent study found that mutation of a Phe located in the S6 domain of HERG decreased block by dofetilide and quinidine (12). However, it is unlikely that a single residue could confer drug sensitivity. Thus, despite the obvious clinical importance of HERG channel block to acquired LQT, the structural basis of the high-affinity drug binding site has not been adequately characterized.

Materials and Methods

Mutagenesis and Channel Expression in Oocytes. Mutations were introduced into the HERG K^+ channel (13) by using site-directed mutagenesis as described previously (14). Complementary RNAs for injection into oocytes were prepared with SP6 Cap-Scribe (Boehringer Mannheim) after linearization of the expression construct with *Eco*RI. Isolation and maintenance of *Xenopus* oocytes and cRNA injection were performed as described previously (14–16).

Voltage Clamp. The two-microelectrode voltage clamp technique (17) was used to record membrane currents in oocytes 2–4 days after cRNA injection as previously described (18). To attenuate endogenous chloride currents, Cl^- was replaced with Mes (2-[*N*-morpholino]ethanesulfonic acid) in the external solution that contained 96 mM NaMes/2 mM KMes/2 mM $CaMes_2$/5 mM Hepes/1 mM $MgCl_2$ adjusted to pH 7.6 with methane sulfonic acid. In some experiments, KMes was increased to 96 mM with a similar reduction in NaMes.

MK-499 was supplied by Merck. Cisapride was purchased from Research Diagnostics Inc. (Flanders, NJ), and terfenadine was purchased from Sigma. Drugs were prepared daily by dilution of a DMSO stock solution kept at −20°C. Drugs were applied with a switching device as described (18). Digitized data were analyzed off-line by using pCLAMP and ORIGIN software.

Molecular Modeling. The 1BL8 KcsA (19) structure was retrieved from the Protein Data Bank. The KcsA structure was used as the template structure for a homology model created by using the MODELER module within INSIGHTII (Ver. 98.0; Molecular Simulations, Burlington, MA). The sequence alignment from Doyle *et al.* (19) was used to generate the homology model. Five homology models were generated by using MODELER. In the area of the cavity, only slight differences were observed, so the first model was used for the docking of MK-499. One hundred low-energy conformations of MK-499 were generated and docked by using the FLOG (Flexible Ligands Oriented on Grid; ref. 20) procedure. One of the docked conformations is shown in Fig. 3. The other high-scoring dockings showed very similar strong π stacking interactions with F656 and Y652.

This paper was submitted directly (Track II) to the PNAS office.

Abbreviations: LQT, long QT syndrome; WT, wild type.

See commentary on page 11683.

†Present address: Department of Cell Physiology and Pharmacology, Maurice Shock Medical Sciences Building, University of Leicester, University Road, Leicester LE1 9HN, U.K.

§To whom reprint requests should be addressed at: Eccles Institute of Human Genetics, University of Utah, 15 N 2030 E Room 4220, Salt Lake City, UT 84112. E-mail: mike.sanguinetti@hci.utah.edu.

The publication costs of this article were defrayed in part by page charge payment. This article must therefore be hereby marked "*advertisement*" in accordance with 18 U.S.C. §1734 solely to indicate this fact.

Article published online before print: *Proc. Natl. Acad. Sci. USA*, 10.1073/pnas.210244497. Article and publication date are at www.pnas.org/cgi/doi/10.1073/pnas.210244497

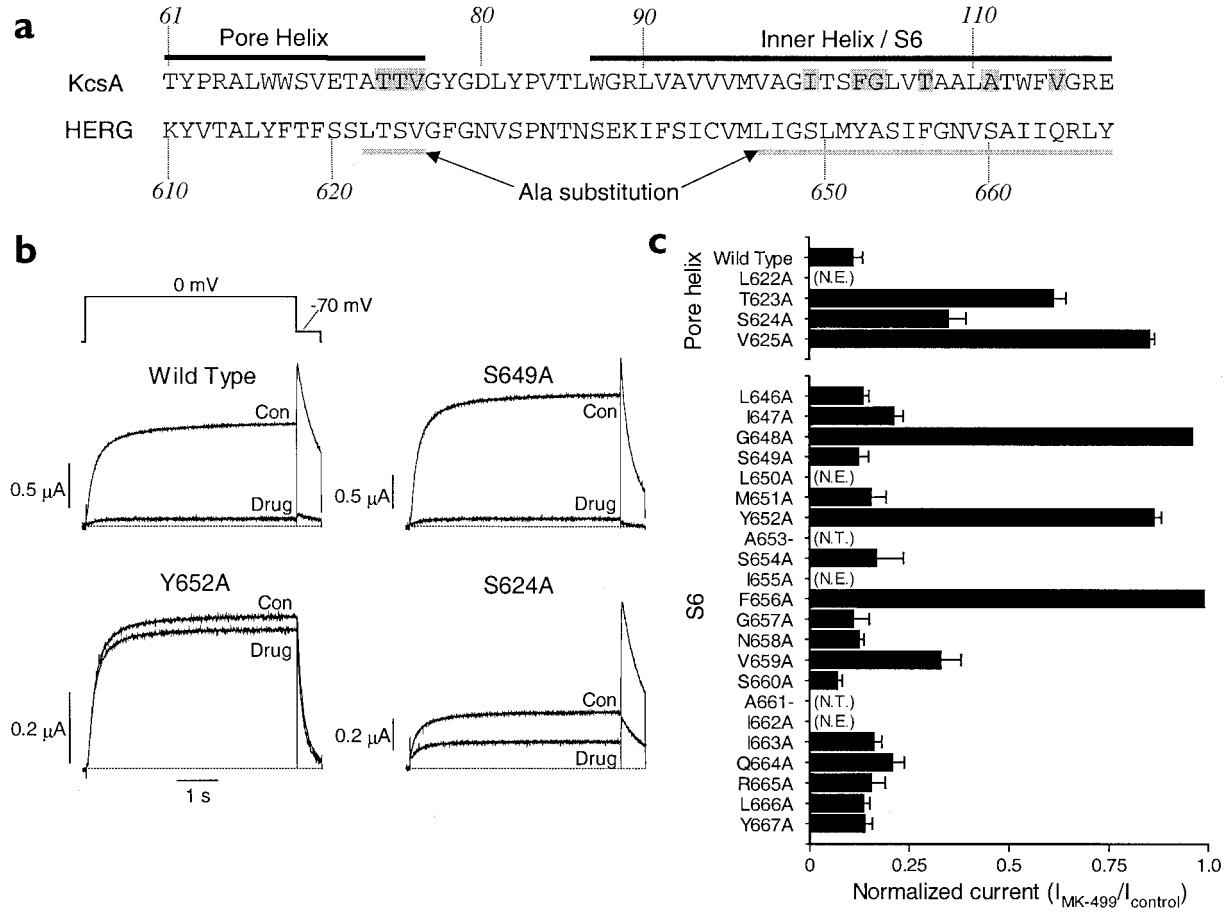

Fig. 1. Alanine-scanning mutagenesis of HERG to define binding sites for MK-499. (*a*) Sequence of the pore helix and inner helix for the KcsA channel (19) and the equivalent residues in the pore helix and S6 transmembrane domain of the HERG K^+ channel. Shaded residues of KcsA face the inside of the inner channel pore. The region of HERG analyzed by Ala-scanning mutagenesis is underlined. (*b*) Block of WT and mutant HERG channel current in oocytes by MK-499. HERG channel currents recorded before (Con) and after (Drug) achieving steady-state block of current with 0.3 μM MK-499. Currents were elicited during 5-s pulses to 0 mV from a holding potential of -90 mV, applied repetitively at 0.166 Hz. (*c*) Normalized current ($I_{MK499}/I_{control}$) measured after steady-state block by 0.3 μM MK-499 ($n = 4-6$; error bars, $\pm$SEM). A value of 1 indicates no detectable decrease in current by the drug. N.T., residues that were not tested; N.E., mutant channels that lacked functional expression.

Results and Discussion

Alanine-scanning mutagenesis was used to determine residues important for block of the HERG channel by MK-499, a methanesulfonanilide antiarrhythmic drug (21). We previously reported that this compound seems to gain access to its binding site on the HERG channel from the intracellular side of the membrane (22), and that this site is located within the cavity and in between the selectivity filter and the activation gate (18). Based on assumed homology with the solved crystal structure of the bacterial KcsA K^+ channel (19), the cavity and inner pore of the HERG channel is lined by the S6 transmembrane domains of four identical subunits that coassemble to form a tetrameric channel. Therefore, we mutated to alanine individual residues of S6 and the few residues of the pore helix predicted to line the channel cavity and inner pore regions (Fig. 1*a*) and determined the sensitivity to block by MK-499 for each mutant channel expressed in *Xenopus* oocytes. Standard two-microelectrode voltage clamp techniques were used to repetitively apply 5-s pulses to 0 mV from a holding potential of -90 mV. A concentration of MK-499 (300 nM) that caused $\approx$85% inhibition of wild-type (WT) HERG current (Fig. 1*b*) was used to assess each mutant channel. As shown in Fig. 1*c*, MK-499 reduced current of most mutant channels in a similar manner to WT HERG. However, three channels with missense mutations located in the S6 domain (G648A, Y652A, and F656A) hardly were affected by 300 nM MK-499. In addition, three channels with a mutation located in the base of the pore helix (T623A, S624A, and V625A) and one located in the S6 domain (V659A) were also less sensitive to MK-499. V659A HERG channel current deactivated much slower than did WT HERG channel current. The resultant decrease in drug trapping (18) could account for the reduced sensitivity of V659A HERG channels to MK-499. A positive shift in the voltage dependence of activation also might decrease the apparent sensitivity of channels to MK-499. However, for T623A, V625A, G648A, Y652A, and F656A HERG, the five mutant channels least affected by drug, values for half-maximal activation were similar or more negative than were WT HERG (Table 1), indicating that decreased sensitivity to drug block was not caused by reduced channel open probability.

To further characterize the relative importance of specific residues to the drug binding site, we determined the concentration–effect relationships for the five mutant channels least affected by drug. The concentration of MK-499 required to block current by 50% (IC_{50}) was 34 nM for WT HERG channels (Fig. 2 *a* and *d*). The IC_{50} for block of Y652A HERG was increased 94-fold relative to WT HERG (Fig. 2 *a* and *d*). Reduction in drug affinity associated with the Y652A mutation was not caused by loss of the hydroxyl side group. Y652F HERG channels having

Table 1. Summary of slope and potentials for half-maximal activation of WT and mutant HERG channels determined from tail current amplitudes fit with Boltzmann function

HERG channel	$V_{0.5}$, mV	*k*, mV	*n*
WT HERG	−16.7 ± 1.3	7.8 ± 0.5	3
T623A	−25.1 ± 1.6	6.7 ± 0.3	4
V625A	−28.9 ± 1.3	7.9 ± 0.3	5
G648A	−33.4 ± 2.5	7.8 ± 0.1	4
Y652A	−18.0 ± 1.4	9.1 ± 1.1	7
F656A	−26.1 ± 2.8	8.2 ± 0.6	3

$V_{0.5}$, potential of half-maximal activation; *k*, slope of the activation curve; *n*, number of oocytes. Currents were activated with 5-s depolarizations from a holding potential of −90 mV.

the conserved mutation of Tyr to Phe (Phe lacks a −OH group) retained normal sensitivity to drug block. The IC_{50} for block of F656A HERG by MK-499 was 22.2 ± 1.9 μM, a 650-fold decrease in sensitivity relative to WT HERG (Fig. 2*d*). Lees-Miller *et al.* (12) also found that mutation of F656 (to Val) reduced the block of HERG by quinidine and dofetilide.

The voltage dependence for fast C-type inactivation (23) of G648A HERG channels was shifted to more negative potentials.

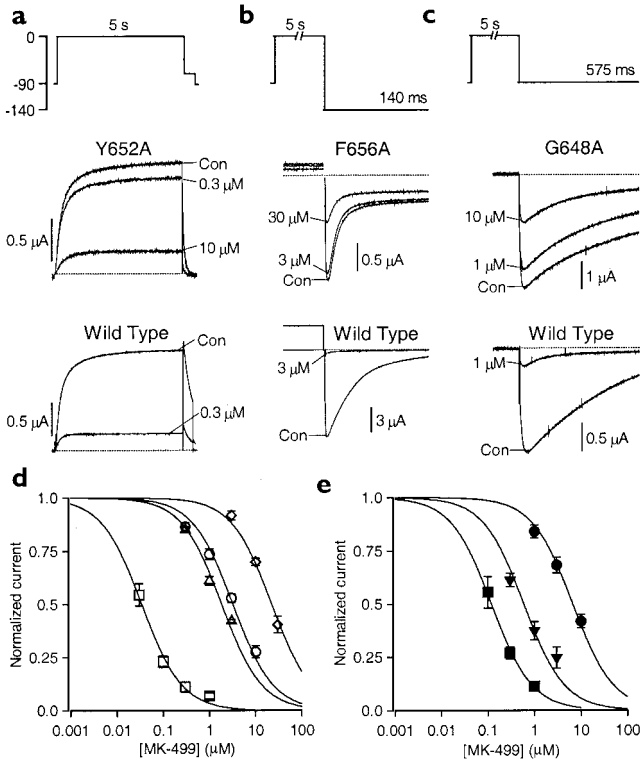

Fig. 2. Concentration-dependent block of WT and mutant HERG channels by MK-499. (*a–c*) Voltage pulse protocol and currents for WT and mutant HERG channels in the presence and absence of indicated concentrations of MK-499. Currents were measured in the presence of 2 mM extracellular K^+ (*a* and *b*) or 96 mM K^+ (*c*). Because F656A HERG expressed poorly in oocytes, the effect of drug on this mutant channel was quantified during pulses to −140 mV after the 5-s activating pulses. (*d*) Concentration–effect relationship for block by MK-499 measured in the presence of 2 mM extracellular K^+. The IC_{50}, determined by using a Hill equation with a coefficient of 1, was 0.034 ± 0.002 μM for WT HERG (□), 1.83 ± 0.2 μM for V625A (△), 3.2 ± 0.34 μM for Y652A HERG (○), and 22.2 ± 1.9 μM for F656A HERG (◇). (*e*) Concentration–effect relationship for block by MK-499 measured in the presence of 96 mM extracellular K^+. The IC_{50} was 0.12 ± 0.005 μM for WT HERG (■), 0.59 ± 0.01 μM for T623A HERG (▼), and 6.6 ± 0.48 μM for G648A HERG (●). *n* = 4–6 for all channels.

This shift necessitated the use of high extracellular K^+ (96 mM KMes) to reduce inactivation (24) and elicit larger currents (Fig. 2*c*). The IC_{50} for WT HERG by using this protocol was 120 ± 5 nM for WT HERG and 6.6 ± 0.48 μM for G648A HERG, a 55-fold increase (Fig. 2*e*). This finding was unexpected because previous studies concluded HERG channel inactivation was required for high-affinity drug block (11, 12), suggesting that enhanced inactivation might increase drug potency.

T623 and V625 are located at the base of the pore helix. The IC_{50} for V625A HERG by MK-499 was 1.6 ± 0.06 μM, a 50-fold increase relative to WT HERG. Not surprisingly, because V625 is located within the K^+ signature sequence of HERG (SVGFG), mutation to Ala reduced the selectivity of the channel for K^+ (data not shown). Like G648A HERG, the voltage dependence of T623A HERG channel inactivation was shifted to more negative potentials. Therefore, the effect of MK-499 on T623A HERG channels was assessed by using the 96 KMes bath solution. Under these conditions, the IC_{50} for T623A HERG was 0.59 ± 0.01 μM, a 5-fold increase relative to WT HERG.

In summary, the rank order of importance of HERG channel residues that affect binding of MK-499 was F656 ≫ Y652 > G648 = V625 > T623 > S624 = V659. Based on homology with KcsA, all three of the residues in S6 that have substantially altered sensitivity to MK-499 (G648A, Y652A, and F656A) are predicted to face toward the inside of the HERG channel pore. G648 is located nearest the pore helix, and Y652 and F656 are each separated by a little more than a single turn of the S6 α helix (Fig. 3*a*). Space-filling models of KcsA (19) indicate that residues located on the N-terminal side of G648 in the S6 domain or to L622 in the pore helix would not be accessible to a large molecule from the channel cavity. Thus, it is unlikely that residues important for drug binding are outside the Ala-scanned region. However, we cannot rule out the possibility of additional binding sites within this region. I662A HERG channels did not functionally express, and Ala-scanning cannot determine the contribution of residues that are already Ala (A653 and A661) and may be a less sensitive test of residues such as Val with a similar hydrophobicity to Ala. In addition, future studies will be required to determine whether MiRP1, an accessory subunit reported to alter kinetics and single-channel conductance of HERG (3), could alter the affinity of drug binding.

Other voltage-gated K^+ channels (Kv1–Kv4) have Ile and Val in the equivalent positions of the aromatic residues Y652 and F656 of HERG, whereas the other residues that most affect MK-499 sensitivity are absolutely (G648 and T623) or strongly (V625) conserved. The amino acid in the equivalent position of S624 is also similar (Thr) in most other voltage-gated K^+ channels. This similarity raises the obvious possibility that high-affinity blockers of HERG channels interact primarily with the aromatic side groups of Y652 and F656. To test this hypothesis, we generated a homology model of HERG by using MODELER in INSIGHTII by using the KcsA crystal structure (19). Multiple energy-accessible conformations of MK-499 were generated and docked into the homology model by using FLOG (20). The docking shown in Fig. 3 shows a π stack to one of the F656 residues with the p-CN phenyl ring. The methanesulfonanilide moiety extends into a pocket formed on one side by G648 and by T623 and S624 on the other side. A π stacking interaction is seen between Y652 and the benzopyran adjacent to the methanesulfonanilide group. In the docking shown, there is no direct interaction with V625; alternate dockings were explored but no direct interactions were seen. This model suggests that mutation of V625 or G648 to Ala disrupts the MK-499 binding site by altering the size or shape of the binding pocket formed between the pore helix and the S6 domain of a single subunit.

Many drugs other than methanesulfonanilides also block HERG, including the gastrointestinal prokinetic agent cisapride (25) and the antihistamine terfenadine (26) (Fig. 4*a*). Because of

PHARMACOLOGY

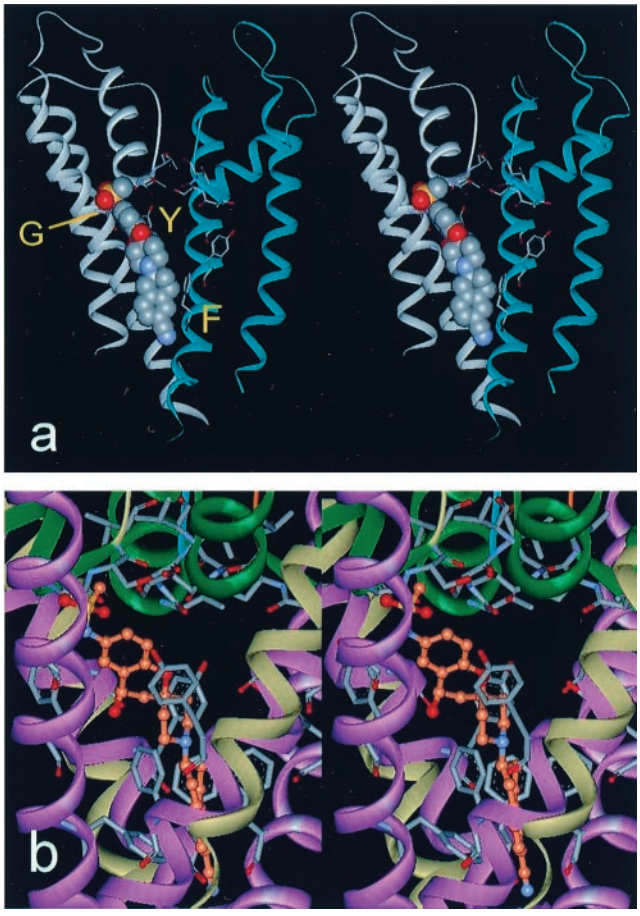

Fig. 3. Docking of a MK-499 molecule within the cavity of the homology model of the HERG K^+ channel. (*a*) Stereoview of the S5-S6 domains of two HERG subunits with docked molecule of MK-499 (shown as a space-filling model). T623, S624, V625, G648, Y652, and F656 are shown as sticks. (*b*) Close-up stereoview of MK-499 in a four-subunit model of the channel. T623, S624, and V625 of the pore helix (green), and G648, Y652, and F656 of the S6 domain (magenta) are shown as sticks; MK-499 is shown as a ball and stick model. Only two of the four S5 domains (yellow) are shown. The homology model of HERG is based on the KcsA (19) channel structure.

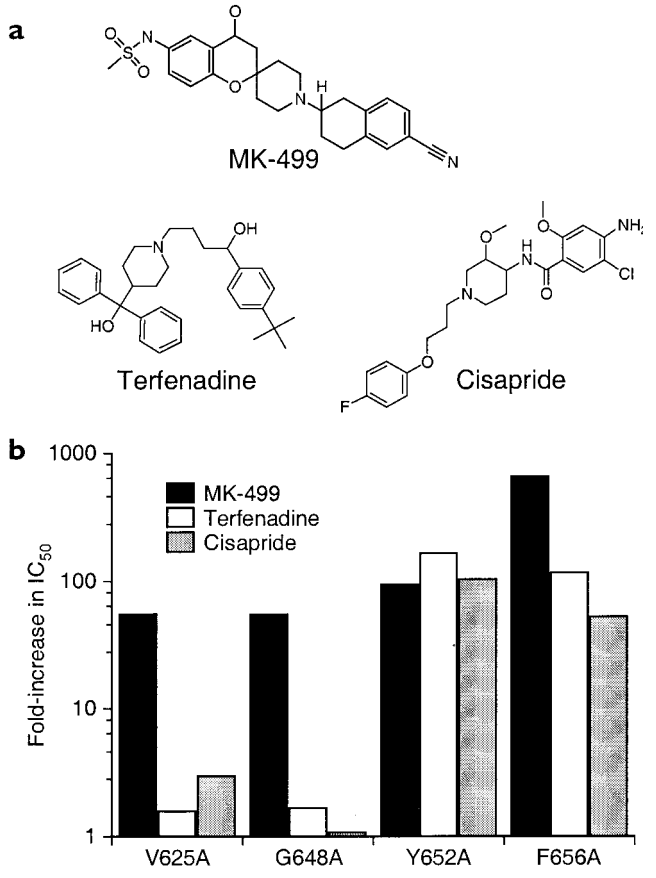

Fig. 4. Mutations of HERG that affect potency for block of HERG channels by MK-499, cisapride, and terfenadine. (*a*) Structures of the three compounds. (*b*) -Fold increase in IC_{50} determined for each mutant channel plotted on a logarithmic scale. The IC_{50} was 0.134 ± 0.019 μM for terfenadine (n = 5) and 0.133 ± 0.011 μM for cisapride (n = 4).

this side effect, both these drugs recently were removed from the market by the Food and Drug Administration. Interaction of these drugs with WT HERG and four mutant HERG channels was assessed by using the same methods described for MK-499. Block of HERG channels by terfenadine and cisapride was relatively unaffected by the two mutations located in (V625A) or near (G648A) the pore helix, but was strongly reduced by mutation of either of the two aromatic amino acids (Y652 and F656) that affect MK-499 binding (Fig. 4*b*). This finding suggests that although cisapride and terfenadine bind within the channel cavity, neither drug binds to the pocket between the pore helix and S6 domain shown to affect interaction with the methanesulfonyl group of MK-499.

Many blockers of Na^+ and Ca^{2+} channels also bind to residues in the S6 domains. These include local anesthetics, class I antiarrhythmics and anticonvulsants that block Na^+ channels, and dihydropyridines and phenylalkamines that block L-type Ca^{2+} channels. For both channel types, molecular determinants for high-affinity drug binding have been identified in the S6 regions of domains III and IV by using Ala-scanning mutagenesis (27–30). Although the drug binding sites are highly complex, there are some similarities with the binding site in HERG. In Na^+ and Ca^{2+} channels, the position of the binding sites are consistent with alignment on an α helical structure, with the sensitive residues facing into the channel cavity. Binding sites for drugs on both channel types include aromatic residues (Phe and Tyr) on S6. For example, F1764A and Y1771A reduce the sensitivity of type IIA Na^+ channels to lidocaine, phenytoin, flecainide, and quinidine (28).

All of the residues in the pore helix and S6 domain of HERG shown here to interact with MK-499 binding are conserved in eag channels. However, the eag channel is relatively insensitive to block by dofetilide (11) and MK-499 (IC_{50} > 10 μM; data not shown). Unlike HERG, eag channels do not inactivate. Therefore, as suggested previously (11, 31), the high-affinity binding site for methanesulfonanilides may be the inactivated state of HERG. However, the insensitivity of eag channels to block by these drugs is not fully explained by the lack of inactivation. G628C/S631C HERG, a channel with a double mutation that completely removes inactivation (23), is still relatively sensitive to MK-499. The IC_{50} for block of G628C/S631C HERG was 336 ± 33 nM (n = 7; data not shown), only about 10 times less sensitive than WT HERG. In the present study, the voltage dependence of inactivation varied for HERG mutants with reduced MK-499 binding affinity. In 2 mM K_o solutions, no outward currents for G648A, T623A, and F656A HERG could be recorded, suggesting a negative shift in the voltage dependence of inactivation. Rectification of Y652A HERG was similar to WT HERG, whereas V625A HERG currents showed no rectification at potentials as high as +60 mV, indicating a removal or large positive shift of inactivation. Thus, factors other

than inactivation must account for the difference in drug sensitivity of eag and HERG channels.

Our findings suggest a possible structural explanation for how many commonly used drugs block HERG channels, but not other voltage-gated channels, to cause acquired LQT. Access of MK-499 and related drugs to the binding site on HERG requires channel opening (32). Closure of the activation gate (deactivation) traps the molecule within the cavity (18), and inactivation can dramatically enhance binding affinity (11, 12) of the drug to the site described here. Other voltage-gated K^+ channels (Kv1–Kv4) contain a Pro-X-Pro sequence in the S6 domain that has been proposed to cause a sharp bend in the S6 helices (33) and may reduce the volume of the channel cavity. The small volume would preclude the trapping of large molecules like MK-499. HERG channels do not have Pro residues in S6 and instead have Ile-Phe-Glu in the equivalent location, where Phe is F656. Most importantly, other voltage-gated K^+ channels (Kv1–Kv4) have Ile and Val (Ile) in the equivalent positions of the aromatic residues Y652 and F656 of HERG. As corroborated in our model of MK-499 interaction with the HERG channel, electrostatic interactions between π electrons and hydrogen atoms of the aromatic rings of Y652/F656 and the drug molecule are crucial for high-affinity binding.

Our model, combined with a structure-activity correlation for chemically related compounds having a variable potency for block of HERG, could be used to develop a virtual screening tool to eliminate compounds that are likely to block HERG channels from further development.

We thank Mike Martines and Diana Lim for technical assistance, and Mark Keating and Scott Rogers for helpful discussions. The study was supported by a Wellcome Trust Prize-Traveling research fellowship to J.S.M. and National Institutes of Health (National Heart, Lung, and Blood Institute) Grant HL55236 to M.C.S.

1. Keating, M. T. & Sanguinetti, M. C. (1996) *Science* **272,** 681–685.
2. Curran, M. E., Splawski, I., Timothy, K. W., Vincent, G. M., Green, E. D. & Keating, M. T. (1995) *Cell* **80,** 795–804.
3. Abbott, G. W., Sesti, F., Splawski, I., Buck, M. E., Lehmann, M. H., Timothy, K. W., Keating, M. T. & Goldstein, S. A. (1999) *Cell* **97,** 175–187.
4. Sanguinetti, M. C., Jiang, C., Curran, M. E. & Keating, M. T. (1995) *Cell* **81,** 299–307.
5. Trudeau, M., Warmke, J. W., Ganetzky, B. & Robertson, G. A. (1995) *Science* **269,** 92–95.
6. Roden, D. M. (1998) *Am. J. Cardiol.* **82,** 49I–57I.
7. El-Sherif, N. & Turitto, G. (2000) in *Cardiac Electrophysiology from Cell to Bedside,* eds. Zipes, D. P. & Jalife, J. (Saunders, Philadelphia), 3rd Ed., pp. 662–673.
8. Roden, D. M., Lazzara, R., Rosen, M., Schwartz, P. J., Towbin, J. & Vincent, G. M. (1996) *Circulation* **94,** 1996–2012.
9. Crumb, W. & Cavero, I. (1999) *Pharmaceut. Sci. Technol.* **2,** 270–280.
10. Pourrias, B., Porsalt, R. D. & Lacroix, P. (1999) *Drug Dev. Res.* **47,** 55–62.
11. Ficker, E., Jarolimek, W., Kiehn, J., Baumann, A. & Brown, A. M. (1998) *Circ. Res.* **82,** 386–395.
12. Lees-Miller, J. P., Duan, Y., Teng, G. Q. & Duff, H. J. (2000) *Mol. Pharmacol.* **57,** 367–374.
13. Warmke, J. W. & Ganetzky, B. (1994) *Proc. Natl. Acad. Sci. USA* **91,** 3438–3442.
14. Sanguinetti, M. C. & Xu, Q. P. (1999) *J. Physiol. (London)* **514,** 667–675.
15. Goldin, A. L. (1991) *Methods Cell Biol.* **36,** 487–509.
16. Goldin, A. L. & Sumikawa, K. (1992) *Methods Enzymol.* **207,** 279–296.
17. Stuhmer, W. (1992) *Methods Enzymol.* **207,** 319–339.
18. Mitcheson, J. S., Chen, J. & Sanguinetti, M. C. (2000) *J. Gen. Physiol.* **115,** 229–240.
19. Doyle, D. A., Morais Cabral, J., Pfuetzner, R. A., Kuo, A., Gulbis, J. M., Cohen, S. L., Chait, B. T. & MacKinnon, R. (1998) *Science* **280,** 69–77.
20. Miller, M. D., Kearsley, S. K., Underwood, D. J. & Sheridan, R. P. (1994) *J. Comput. Aided Mol. Des.* **8,** 153–174.
21. Lynch, J. J., Wallace, A. A., Stupienski, R. F., 3rd, Baskin, E. P., Beare, C. M., Appleby, S. D., Salata, J. J., Jurkiewicz, N. K., Sanguinetti, M. C., Stein, R. B., *et al.* (1994) *J. Pharmacol. Exp. Ther.* **269,** 541–554.
22. Zou, A., Curran, M. E., Keating, M. T. & Sanguinetti, M. C. (1997) *Am. J. Physiol.* **272,** H1309–H1314.
23. Smith, P. L., Baukrowitz, T. & Yellen, G. (1996) *Nature (London)* **379,** 833–836.
24. Wang, S., Morales, M. J., Liu, S., Strauss, H. C. & Rasmusson, R. L. (1996) *FEBS Lett.* **389,** 167–173.
25. Mohammad, S., Zhou, Z., Gong, Q. & January, C. T. (1997) *Am. J. Physiol.* **42,** H2534–H253.
26. Roy, M.-L., Dumaine, R. & Brown, A. M. (1996) *Circ. Res.* **94,** 817–823.
27. Hockerman, G. H., Johnson, B. D., Scheuer, T. & Catterall, W. A. (1995) *J. Biol. Chem.* **270,** 22119–22122.
28. Ragsdale, D. S., McPhee, J. C., Scheuer, T. & Catterall, W. A. (1996) *Proc. Natl. Acad. Sci. USA* **93,** 9270–9275.
29. Hockerman, G. H., Johnson, B. D., Abbott, M. R., Scheuer, T. & Catterall, W. A. (1997) *J. Biol. Chem.* **272,** 18759–18765.
30. Peterson, B. Z., Johnson, B. D., Hockerman, G. H., Acheson, M., Scheuer, T. & Catterall, W. A. (1997) *J. Biol. Chem.* **272,** 18752–18758.
31. Wang, S., Morales, M. J., Liu, S., Strauss, H. C. & Rasmusson, R. L. (1997) *FEBS Lett.* **417,** 43–47.
32. Spector, P. S., Curran, M. E., Keating, M. T. & Sanguinetti, M. C. (1996) *Circ. Res.* **78,** 499–503.
33. del Camino, D., Holmgren, M., Liu, Y. & Yellen, G. (2000) *Nature (London)* **403,** 321–325.